

Selective Hg²⁺ Sensing Behaviors of Rhodamine Derivatives with Extended Conjugation Based on Two Successive Ring-Opening Processes

Chunyan Wang^{†,‡} and Keith Man-Chung Wong^{*,†,‡}

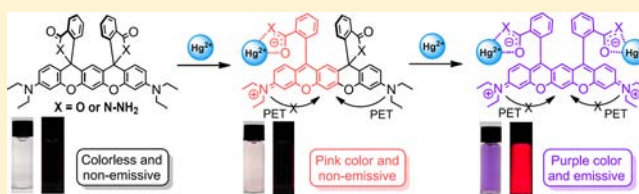
[†]Department of Chemistry, South University of Science and Technology of China, No. 1088, Tangchang Boulevard, Nanshan District, Shenzhen, Guangdong, P.R. China

[‡]Department of Chemistry, The University of Hong Kong, Pokfulam Road, Hong Kong, P.R. China

S Supporting Information

ABSTRACT: A novel class of rhodamine derivatives with two spiroactam moieties have been synthesized, and their two stereoisomers of *cis*- and *trans*-forms have been successfully separated and isolated, as well as structurally characterized by X-ray crystallography. Attributed to the successive ring-openings of two spiroactam moieties, different solution color, electronic absorption and emission responses were exhibited upon addition of various concentrations of mercury-

(II) ion. Arising from two successive ring-opening processes in the presence of various concentration of Hg(II) ion, two reporting states with different spectroscopic properties were suggested, that is, the first state showing pink color (absorption maximum at 496 nm) but no emission, while the second state giving purple color (absorption maximum at 593 nm) and red emission (emission maximum at 620 nm). The mechanism of such different spectroscopic responses was also proposed and has also been supported by computational studies. An extension of the present work to the study of the corresponding chemodosimeters from the compounds with two spiroactam groups has been made, in which a stoichiometric and irreversible Hg(II)-promoted reaction of thiosemicarbazides was utilized to form 1,3,4-oxadiazoles.



INTRODUCTION

Since the pioneering works of Pedersen, Lehn, and Cram¹ on the design and syntheses of cation-selective crown ethers, cryptands, and spherands, studies on the host–guest interactions of known chemical composition and structure are indeed highly interesting and useful. Conventional approaches to chemosensors have commonly made use of a “lock-and-key” design, wherein a specific receptor is synthesized to strongly and highly selectively bind the analyte of interest.² The development of optical signaling systems for various chemosensors to detect different types of analyte has received considerable attention in the past few decades. Design of sensors based on changes in luminescence is a promising field and appears to be particularly attractive because of their simplicity, high sensitivity, high selectivity, and instantaneous response by simple luminescence enhancement or quenching.³ Numerous excellent studies focus on the development of luminescent chemosensors for various analyses of transition- or heavy-metal ions such as Hg²⁺, Pb²⁺, Zn²⁺, and Cu²⁺ owing to their fundamental role in a wide range of chemical, biological, and environmental processes.⁴

Rhodamine-based dyes have been widely used in the past several decades since the first report on the preparation of rhodamine in 1905.^{5a} It is well-known that many derivatives of rhodamine are in equilibrium^{5b} between two constitutional isomers with completely different spectroscopic properties. The

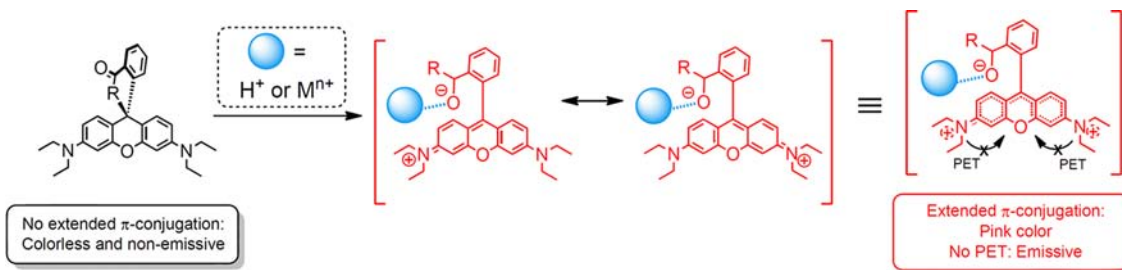
ring-closed spiroactam form is colorless and nonfluorescent, while the ring-opened amide form displays intense pink to red color and strong fluorescence. Various rhodamine-based turn-on fluorescent probes for metal cations or oxidative species have been reported in the past few years.^{6–9} Depending on the nature of functional groups attached to the spiroactam, such fluorescent probes were found to selectively bind to various metal cations, in particular for the sensing of mercury(II) ion. In general, the sensing mechanism of these probes is based on the structural modulation from the spiroactam to the open-cycle form. Upon addition of analytes, a drastic color change from colorless to intense color with a concomitant appearance of strong fluorescence will result from the spirocycle opening process through a reversible coordination or an irreversible chemical reaction with the rhodamine probe. Because of the resonance structure of the rhodamine, in which the two amino groups are partially positive-charged, any emission quenching through the possible photoinduced electron transfer (PET) would not be possible (Scheme 1). As a result, the ring-opening would lead to the intense absorption band and emission in the visible region.

For the ordinary rhodamine derivatives having only one spiroactam group for the ring-opening process, their

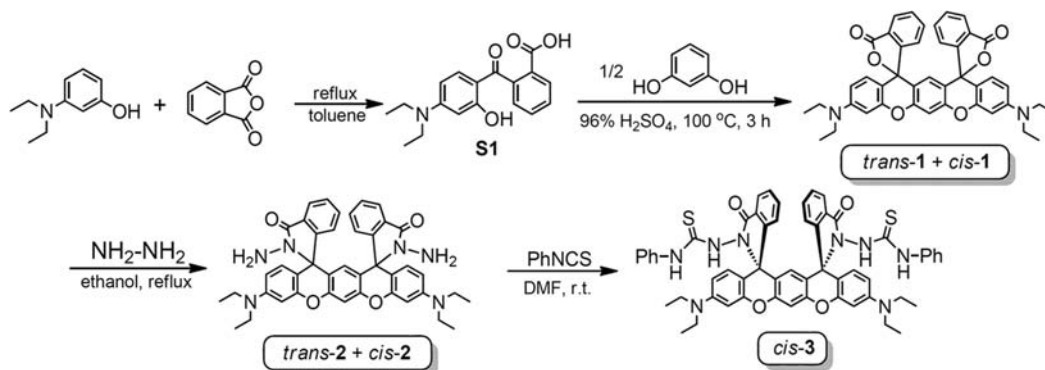
Received: July 14, 2013

Published: November 11, 2013

Scheme 1. Drastic Color Change and Emission Enhancement Arising from the Ring-Opening of Spirolactam Group



Scheme 2. Synthetic Route of 1–3



absorption and emission colors are mainly dependent on the substituents on the amino groups with limited energy variations. Herein we report the design and synthesis of a novel class of rhodamine derivatives, **1** and **2**, in which there are two spirolactam groups with five fused six-membered rings (Scheme 2). Two stereoisomers of *cis*- and *trans*-forms have been successfully separated, isolated, as well as structurally characterized by X-ray crystallography. Mercury(II) ion was found to selectively induce ring-opening of the spirolactam groups. In view of the different extent of the π -conjugation upon successive ring-opening processes, different solution color, electronic absorption, and emission responses were exhibited in the presence of various concentrations of mercury(II) ions. An extension of the present work to the study of the corresponding chemodosimeters from the compounds with two spirolactam groups has been made, *cis*-**3** (Scheme 2), in which a stoichiometric and irreversible Hg(II)-promoted reaction of thiosemicarbazides was utilized to form 1,3,4-oxadiazoles.

EXPERIMENTAL SECTION

Materials and Reagents. All the solvents for synthesis were of analytical grade. Methanol for analysis was of HPLC grade. 3-(Diethylamino)phenol, phthalic anhydride, hydrazine monohydrate, and resorcinol were purchased from Aldrich Chemical Co. Magnesium(II) perchlorate, calcium(II) perchlorate tetrahydrate, barium(II) perchlorate, lithium perchlorate, sodium perchlorate, potassium perchlorate, iron(II) perchlorate, cobalt(II) perchlorate, nickel(II) perchlorate, mercury(II) perchlorate, silver(I) perchlorate, and lead(II) perchlorate hydrate were purchased from Aldrich Chemical Co. with purity over 99.0% and were used as received.

Synthesis. *Synthesis of cis-1 and trans-1.* To a solution of 3-diethylaminophenol (2.0 g, 12 mmol) in toluene (60 mL) was added phthalic anhydride (1.8 g, 12 mmol). The suspension was heated to reflux for 6 h. The resulting residue was washed with methanol to provide the intermediate **S1** (2.1 g, 55%). To a mixture of **S1** (2.5 g, 8.0 mmol) and resorcinol (0.44 g, 4.0 mmol) was added concentrated

sulfuric acid (10 mL) dropwise at 0 °C. The resulting suspension was heated at 100 °C for 3 h. After the mixture was cooled down to room temperature and poured into ice water (100 mL) with vigorous stirring, the pH of the mixture was adjusted to ~ 7 . The mixture was extracted with dichloromethane (20 mL) three times. The organic layers were dried over anhydrous magnesium sulfate and evaporated to give the crude product of the mixture of *cis*-**1** and *trans*-**1** (1.43 g, 54%). The purification and separation of the stereoisomer were achieved by silica column chromatography eluting with dichloromethane and methanol (150:1) to give the pure form of *cis*-**1** and *trans*-**1** as a white solid in the ratio of about 1:1. Subsequent recrystallization of the respective compounds by diffusion of diethyl ether vapor into a solution of the product in dichloromethane afforded *cis*-**1** and *trans*-**1** as white crystals, respectively. *cis*-**1**: ¹H NMR (300 MHz, CDCl₃) δ 7.83–7.80 (2H, m), 7.46–7.39 (4H, m), 7.13 (1H, s), 6.93–6.90 (2H, m), 6.48 (2H, d, $J = 8.9$ Hz), 6.48 (2H, d, $J = 2.5$ Hz), 6.32 (2H, dd, $J = 2.5$ Hz, $J = 8.9$ Hz), 5.98 (1H, s), 3.35 (8H, q, $J = 7.0$ Hz), 1.17 (12H, t, $J = 7.0$ Hz). ¹³C NMR (100 MHz, CDCl₃) δ 169.0, 153.4, 153.2, 152.2, 149.8, 134.2, 129.4, 128.8, 128.6, 127.4, 125.0, 123.5, 116.4, 108.6, 105.2, 104.4, 97.8, 83.4, 44.6, 12.6. HRMS (EI) for C₄₂H₃₆N₂O₆ (M⁺): calcd 664.2573, Found: 664.2550. *Trans*-**1**: ¹H NMR (300 MHz, CDCl₃) δ 7.79–7.77 (2H, d, $J = 7.6$ Hz), 7.63–7.58 (2H, m), 7.53–7.48 (2H, m), 7.14–7.11 (3H, m), 6.50–6.47 (4H, m), 6.32 (2H, dd, $J = 2.4$ Hz, $J = 8.9$ Hz), 6.03 (1H, s), 3.36 (8H, q, $J = 7.0$ Hz), 1.17 (12H, t, $J = 7.0$ Hz). ¹³C NMR (75 MHz, CDCl₃) δ 169.3, 153.3, 153.0, 152.1, 149.8, 135.1, 129.8, 128.8, 127.8, 126.8, 124.6, 124.1, 116.4, 108.6, 105.1, 104.2, 97.8, 83.6, 44.6, 12.6. HRMS (EI) for C₄₂H₃₆N₂O₆ (M⁺): calcd 664.2573, Found: 664.2564.

Synthesis of cis-2 and trans-2. To a suspension of crude product of the mixture of *cis*-**1** and *trans*-**1** (0.5 g, 0.75 mmol) in ethanol (20 mL) was added hydrazine (1.2 mL). The resulting suspension was refluxed overnight. After the resulting suspension was cooled to room temperature, the solvent was removed. To the residue was added deionized water (10 mL). The aqueous phase was extracted with dichloromethane (20 mL) three times. The organic phase was dried by anhydrous magnesium sulfate. The solvent was removed to give the crude product of *cis*-**2** and *trans*-**2** (0.493 g, 94%) in the ratio of about 1:1. The purification and separation of the stereoisomer were achieved by silica column chromatography eluting with dichloromethane and methanol (80:1) to give the pure form of *cis*-**2** and *trans*-**2** as a white

solid after removal of solvent. Subsequent recrystallization of the respective compounds by diffusion of diethyl ether vapor into a solution of the product in dichloromethane afforded *cis-2* and *trans-2* as a white crystal respectively. *cis-2*: ^1H NMR (400 MHz, CDCl_3), δ 7.82–7.80 (2H, m), 7.44–7.42 (4H, m), 7.09 (1H, s), 7.01–6.99 (2H, m), 6.44 (2H, d, $J = 2.5$ Hz), 6.34 (2H, d, $J = 8.9$ Hz), 6.27 (2H, dd, $J = 2.5$ Hz, $J = 8.9$ Hz), 5.97 (1H, s), 3.46 (4H, s), 3.33 (8H, q, $J = 7.0$ Hz), 1.16 (12H, t, $J = 7.0$ Hz). ^{13}C NMR (100 MHz, CDCl_3), δ 166.5, 153.4, 150.8, 149.1, 133.0, 129.3, 128.9, 127.7, 126.3, 123.5, 123.3, 115.9, 108.6, 104.9, 104.4, 98.2, 65.4, 44.5, 12.7. HRMS (EI) for $\text{C}_{42}\text{H}_{40}\text{N}_6\text{O}_4$ (M^+): calcd 692.3111, Found: 692.3122. *trans-2*: ^1H NMR (400 MHz), δ 7.74 (2H, d, $J = 7.5$ Hz), 7.31–7.29 (2H, m), 7.27–7.25 (2H, m), 7.07 (1H, s), 6.81 (2H, d, $J = 7.5$ Hz), 6.45 (2H, d, $J = 2.5$ Hz), 6.33 (2H, d, $J = 8.8$ Hz), 6.27 (2H, d, $J = 2.5$ Hz, $J = 8.8$ Hz), 5.87 (1H, s), 3.66 (4H, s), 3.34 (8H, q, $J = 7.0$ Hz), 1.16 (12H, t, $J = 7.0$ Hz). ^{13}C NMR (100 MHz, CDCl_3), δ 166.2, 153.6, 153.4, 150.5, 149.0, 132.2, 129.8, 128.2, 127.9, 127.5, 123.3, 123.0, 115.9, 108.5, 104.6, 104.3, 98.0, 65.3, 44.4, 12.7. HRMS (EI) for $\text{C}_{42}\text{H}_{40}\text{N}_6\text{O}_4$ (M^+): calcd 692.3111, Found: 692.3110.

Synthesis of *cis-3*. The mixture of **2** (346 mg, 0.5 mmol) and phenyl isothiocyanate (300 μL , 2.47 mmol) in dimethylformamide (DMF, 3 mL) was stirred at room temperature for 24 h under nitrogen. The solvent was removed, and the crude product was purified by silica column chromatography eluting with dichloromethane and methanol (100:1) to give the crude product as a light purple solid after removal of solvent. Subsequent recrystallization of the compound by diffusion of diethyl ether vapor into a solution of the crude product in dichloromethane afforded pure *cis-3* (221 mg, yield 46%). ^1H NMR (400 MHz, CDCl_3), δ 7.78–7.76 (2H, m), 7.52–7.47 (4H, m), 7.24 (2H, s), 7.19 (1H, s), 7.19–7.13 (4H, m), 7.11–7.08 (2H, m), 6.96–6.94 (4H, m), 6.81 (2H, m), 6.64 (2H, s), 6.58 (2H, d, $J = 2.6$ Hz), 6.42 (2H, d, $J = 8.8$ Hz), 6.29 (2H, dd, $J = 2.6$ and 8.9 Hz), 5.69 (1H, s), 3.40–3.30 (8H, m), 1.18–1.15 (12H, m). ^{13}C NMR (100 MHz, CDCl_3) δ 183.0, 166.5, 154.3, 154.0, 149.8, 148.4, 137.5, 135.0, 129.7, 128.7, 128.6, 127.6, 126.6, 125.5, 124.3, 123.8, 115.8, 109.2, 105.6, 103.2, 98.5, 66.5, 44.6, 12.6. FAB-MS: 963 [$\text{M} + \text{H}$] $^+$. Elemental analyses calcd for $\text{C}_{56}\text{H}_{50}\text{N}_8\text{O}_4\text{S}_2 \cdot 1/2\text{CH}_2\text{Cl}_2 \cdot 1/2\text{H}_2\text{O}$ (found): C 66.88 (67.00), H 5.17 (4.94), N 11.04 (11.34).

Synthesis of **4.** The mixture of **3** (50 mg, 0.052 mmol) and $\text{Hg}(\text{ClO}_4)_2$ (44 mg, 0.11 mmol) in acetonitrile (15 mL) was stirred at room temperature for 20 min. The color of the solution turned to purple-blue. The solvent was removed, and the crude product was purified by silica column chromatography eluting with dichloromethane and methanol (50:1) to afford the desired product as a blue solid (42 mg, 90%) after removal of solvent. Subsequent recrystallization of the compound by diffusion of diethyl ether vapor into a solution of the crude product in dichloromethane afforded pure product. ^1H NMR (400 MHz, acetone- d_6) δ 9.49 (2H, s), 8.04 (2H, dd, $J = 0.8$ and 8.0 Hz), 8.02 (1H, s), 7.84 (2H, td, $J = 1.2$ and 7.6 Hz), 7.77 (2H, td, $J = 1.2$ and 7.6 Hz), 7.54–7.49 (8H, m), 7.40–7.36 (4H, m), 7.30–7.26 (4H, m), 7.03–6.98 (3H, m), 4.08 (4H, q, $J = 7.2$ Hz), 4.00 (4H, q, $J = 7.2$ Hz), 1.50 (6H, t, $J = 7.2$ Hz), 1.37 (6H, t, $J = 7.2$ Hz). ^{13}C NMR (100 MHz, acetone- d_6) δ 160.8, 160.4, 159.8, 157.7, 157.0, 155.9, 139.1, 134.4, 132.3, 132.1, 131.9, 130.6, 129.9, 129.5, 128.8, 123.9, 123.3, 120.9, 120.7, 118.2, 106.1, 99.6, 48.8, 48.6, 13.8, 13.0. FAB-MS: 448.3 [M] $^{2+}$, 895.3 [$\text{M} - \text{H}$] $^+$. Elemental analyses calcd for $\text{C}_{56}\text{H}_{48}\text{Cl}_2\text{N}_8\text{O}_{12} \cdot \text{CH}_2\text{Cl}_2 \cdot \text{H}_2\text{O}$ (found): C 57.10 (57.32), H 4.34 (4.07), N 9.35 (9.56).

Physical Measurements and Instrumentation. ^1H and ^{13}C NMR spectra were recorded at room temperature on a Bruker AVANCE DPX 300 (300 MHz for ^1H and 75 MHz for ^{13}C) or 400 (400 MHz for ^1H and 100 MHz for ^{13}C) Fourier-transform NMR spectrometers. ^1H NMR chemical shifts were reported in ppm using CDCl_3 (δ_{H} 7.26 ppm) or $(\text{CD}_3)_2\text{CO}$ (δ_{H} 2.05 ppm) as internal standard. ^{13}C NMR chemical shifts were reported in ppm relative to CDCl_3 (δ_{C} 77.16 ppm) or $(\text{CD}_3)_2\text{CO}$ (δ_{C} 29.8 ppm). High resolution EI mass spectra were recorded on a Thermo Scientific DFS High Resolution Magnetic Sector mass spectrometer. The electronic absorption spectra were obtained using a Hewlett-Packard 8452A diode array spectrophotometer. Steady state excitation and emission

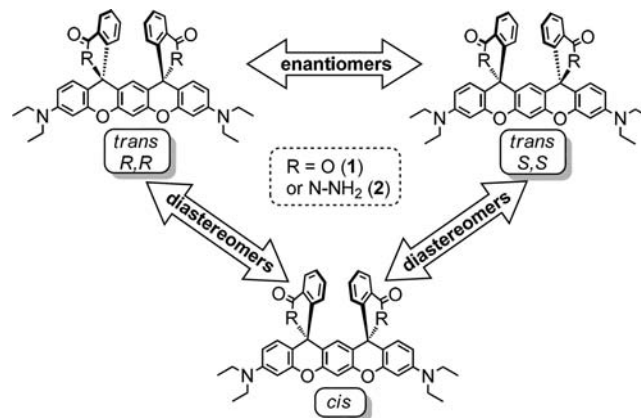
spectra at room temperature were recorded on a Spex Fluorolog-3 Model FL3-211 fluorescence spectrofluorometer equipped with a R2658P PMT detector. The solution samples for the electronic absorption and emission titration experiments were in the concentration range from 9.57×10^{-6} to 1.79×10^{-5} M. Elemental analyses of complexes were performed on a Flash EA 1112 elemental analyzer at the Institute of Chemistry, Chinese Academy of Sciences.

Theoretical and Computational Methodology. All computations were done with the Gaussian09 program package¹⁰ with different parameters for structure optimizations and vibrational analysis. The singlet ground-state geometries were fully optimized with Becke's three-parameter exchange functional along with the Lee–Yang–Parr correlation functional with the restricted (B3LYP) at the standard split valence plus polarization function 6-31G(d) basis set.⁸¹ The fully optimized stationary points were further characterized by harmonic vibrational frequency analysis to ensure that real local minima had been found that had no imaginary vibrational frequencies. The electronic absorption spectra were calculated using the time-dependent density functional theory (TD-DFT) method with B3LYP/6-31G(d) at the optimized ground state structures. The polarizable continuum model (PCM) was adopted in the TD-DFT calculation of the absorption spectra in the solvent (methanol for the partially and fully ring-opened *cis-1* and acetonitrile for **4** and rhodamine 6G_oxadiazole).

■ RESULT AND DISCUSSIONS

Syntheses and Characterizations. The synthetic methodology is shown in Scheme 2. Reaction of resorcinol and 2-(4-diethylamino-2-hydroxybenzoyl)benzoic acid in concentrated sulfuric acid under reflux condition afforded compound **1**.¹¹ Formation of **2** was achieved from the subsequent reaction of **1** and hydrazine. As revealed from their ^1H NMR spectra of both **1** and **2**, the existence of two diastereomers of *cis*- and *trans*-forms in about 1:1 ratio were found, which can be successfully separated and isolated by column chromatography. A mixture of *cis-2* and *trans-2* in 1:1 ratio was obtained even from pure isomer of *cis-1* or *trans-1*, indicating that the transformation of ester to amide group may involve the ring-opening of the spiro lactam moiety. On the other hand, there are two enantiomers, *R,R* and *S,S*, for each of the diastereomer of *trans*-form (Scheme 3). No attempt has been made to separate

Scheme 3. Diastereomers and Enantiomers of **1** and **2**



such two enantiomers. All of them (*cis-1*, *trans-1*, *cis-2*, and *trans-2*) have been characterized by ^1H NMR, ^{13}C NMR, and HR (EI) mass spectrometry. Single crystals of *cis-1*, *trans-1*, *cis-2*, and *trans-2* suitable for X-ray crystallographic studies were obtained by the slow diffusion of diethyl ether vapor into a concentrated dichloromethane solution of the corresponding

compounds. The molecular structures of two pairs of stereoisomers have also been confirmed by X-ray crystallography (Supporting Information, Figure S1).¹² With the aid of 2D ¹H-¹H COSY NMR results, the assignment of all resonance signals of individual compounds has been established, and their corresponding ¹H NMR spectra showing the aromatic region in CDCl₃ are depicted in Figure 1. The chemical shifts for the

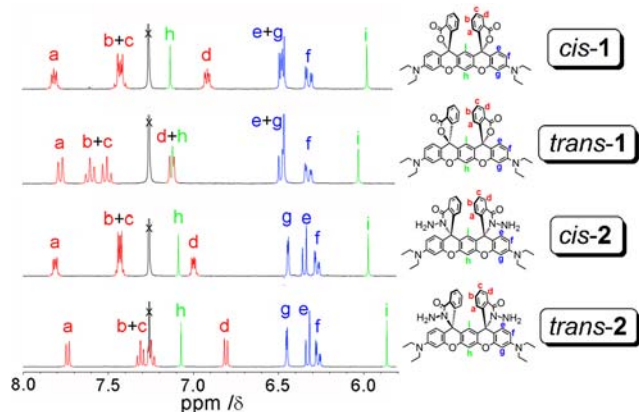


Figure 1. ¹H NMR spectra (right) of *cis*-1 (a), *trans*-1 (b), *cis*-2 (c), and *trans*-2 (d) in CDCl₃ showing the assignment of aromatic resonances.

same proton in their *cis*- and *trans*-forms are different, suggestive of the nature of chemically nonequivalent environments imparted by the change of the relative spatial orientation in the stereoisomers. Compound *cis*-3 was obtained by the reaction of **2** (mixture of *trans*-2 and *cis*-2) and isothiocyanatobenzene. It is interesting to note that reaction from the pure form of *trans*-2 or *cis*-2 as the starting material also afforded compound *cis*-3 in only one configuration of *cis*-form. For characteristic peaks of the quaternary carbon of spirolactam in *cis*-1 (83.4 ppm), *trans*-1 (83.6 ppm), *cis*-2 (65.4 ppm), *trans*-2 (65.3 ppm), *cis*-3 (66.5 ppm) as shown in ¹³C NMR spectra suggested the existence of closed forms in the solution.

Because of the centrosymmetric space groups of *Pbcn* and *P2₁/n*, two enantiomers of *trans*-1 and *trans*-2 were cocrystallized as a racemic mixture, respectively. In general, the five six-membered rings consisting of alternating three benzene and two pyran rings fuse together to form a planar structure, which is the analogue to a pentacene molecule. The planes of 3*H*-isobenzofuran-1-one in **1** and 2-amino-2,3-dihydro-1*H*-isoindol-1-one in **2** are orthogonal to the plane of the five fused ring with the dihedral angles of 85.497–89.441°. In the *trans*-form, the two 3*H*-isobenzofuran-1-one (in **1**) or 2-amino-2,3-dihydro-1*H*-isoindol-1-one (in **2**) groups face opposite directions with the interplanar angles of 11.405–14.056°. On the other hand, the two planes in the *cis*-form are pointing to the same direction with the interplanar angles of 5.549–9.728°.

Hg(II) Ion Sensing. Compounds **1** and **2** are colorless and nonemissive in their solution state. No observable electronic absorption band could be found in the visible region, indicative of the ring closure nature in the spirolactam groups. Selective sensing behaviors of **1** and **2** were investigated for various alkali and alkaline-earth as well as transition metal cations. Solutions of **1** or **2** in methanol exhibit drastic color changes selectively in the presence of Hg²⁺ with no observable color change for K⁺, Na⁺, Li⁺, Ca²⁺, Mg²⁺, Ba²⁺, Pb²⁺, Cd²⁺, Zn²⁺, Co²⁺, Ni²⁺, Ag⁺, Fe²⁺, Cu²⁺. Figure 2 shows the selectivity study of *cis*-2 in

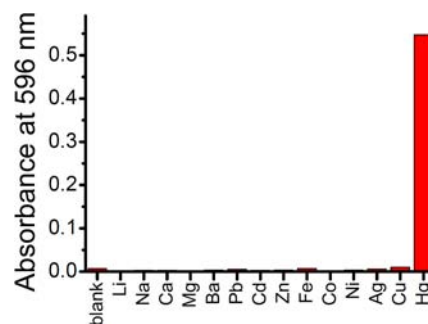


Figure 2. Selectivity study of *cis*-2 (conc. = 1.0×10^{-5} M) in MeOH upon addition of various metal ions (8 mol equiv).

MeOH upon addition of various metal ions. Such selective color change suggests that **1** or **2** can serve as a “naked-eye” indicator for Hg(II) ion. It is interesting to note that the solution color of **1** or **2** changes from colorless to pink without observable emission in the presence of a small amount of Hg(II) ion. Upon further addition of excess amount of Hg(II) ion, the pink solution changes to purple color and an intense red-color emission was observed. Figure 3 shows the solution



Figure 3. Photographs showing the color changes (left) and emission enhancement (right) in the absence of Hg(II) ion for *cis*-2 (a) and *trans*-2 (d), and in the presence of 1.5 equiv of Hg(II) ion for *cis*-2 (b) and *trans*-2 (e) and in the presence of excess amount of Hg(II) ion for *cis*-2 (c) and *trans*-2 (f) in MeOH.

color and emission changes of *cis*-2 and *trans*-2 with Hg(II) ion as the representative example, while the corresponding solution color and emission changes of *trans*-1 are shown in Supporting Information, Figure S2. Both **1** and **2** were found to exhibit the corresponding responses of color and emission changes instantaneously upon the addition of Hg(II) ion.

Spectroscopic Titrations for Hg(II) Ion. Electronic absorption and emission titration studies of **1** and **2** (both in *cis*- and *trans*-forms) with various concentrations of Hg(II) ion were carried out to investigate the profiles of the spectroscopic changes. Both the *cis*-1 and *trans*-1 exhibit essentially the same spectroscopic responses upon addition of Hg(II) ion, indicating that the ring-opening behaviors of stereoisomers of **1** are almost the same. The corresponding electronic absorption spectral changes of *cis*-1 in methanol are illustrated in Figure 4 (left) (Supporting Information, Figure S3 for *trans*-1). Initial addition of Hg(II) ion resulted in an emergence of the absorption bands at 464, 496, and 530 nm, which is responsible for the pink color change. Two well-defined isosbestic points at 288 and 332 nm are observed, indicative of a clean conversion. Such growth of absorption bands reaches a saturation at about 1.7 equiv of Hg(II) ion (Figure 4 (left, inset). On the basis of the occurrence of similar absorption energy for rhodamine derivatives containing three fused rings of a xanthene moiety, the observed absorption bands are ascribed to the ring-opening of one spirolactam group. Further addition of Hg(II) ion resulted in additional absorption bands at 546 and 593 nm, and the absorbance of this 593 nm absorption band increases drastically with the saturation at 80 equiv of Hg(II) ion (Figure

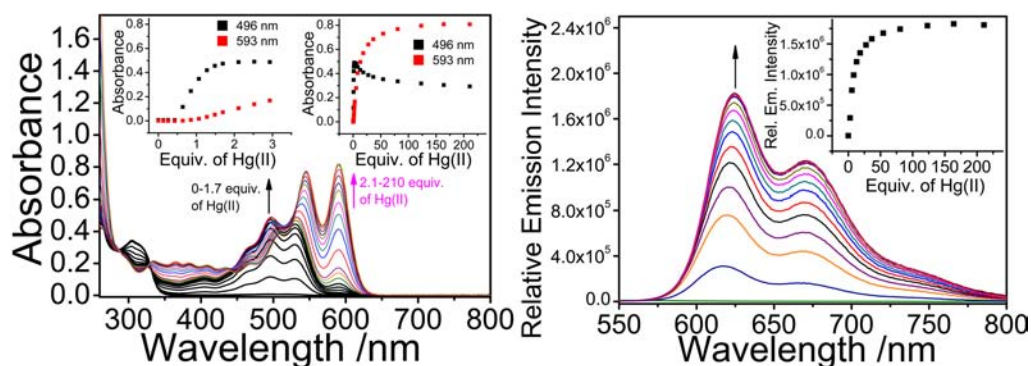


Figure 4. Electronic absorption (left) and emission (right) spectral changes of *cis-1* (conc. = 1.19×10^{-5} M) in MeOH in the presence of various concentrations of Hg(II) ion. Insets show the plot of absorbance or emission intensity as a function of the concentration of Hg(II) ion.

Scheme 4. Proposed Mechanism for the Color Changes and Emission Behaviors of 1 and 2

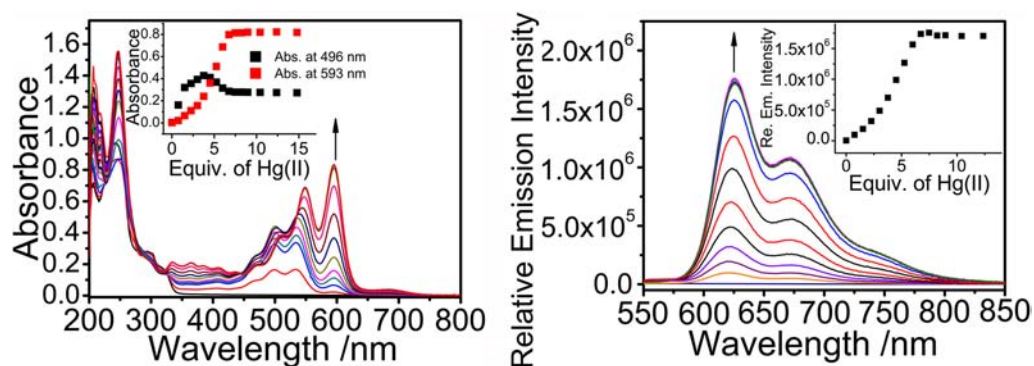
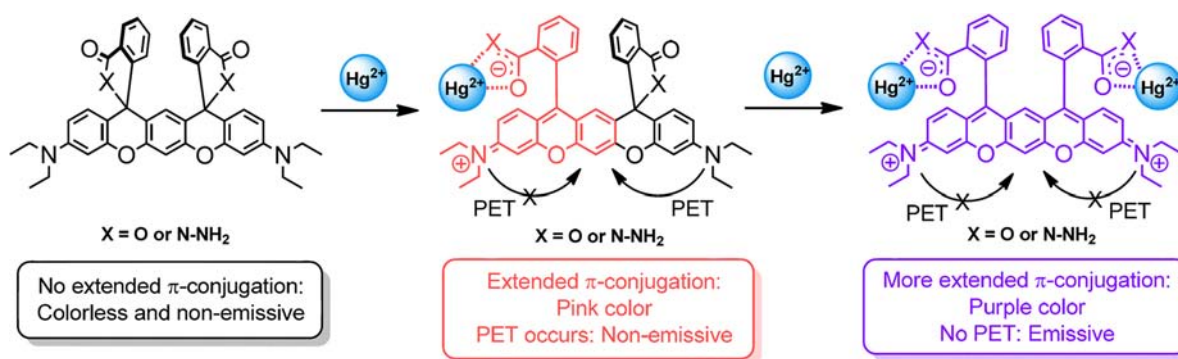


Figure 5. Electronic absorption (left) and emission (right) spectral changes of *cis-2* (conc. = 1.01×10^{-5} M) upon addition of various concentrations of Hg(II) ion in MeOH. Insets show the plot of absorbance or emission intensity as a function of the concentration of Hg(II) ion.

4 (left)). The observation of additional new absorption bands at 546 and 593 nm is reasonably attributed to another ring-opening process of the second spirolactam group since an extension of the π -conjugation across the fused-structure of five rings is anticipated to shift the absorption to the red.

It is noteworthy that an intense vibronic-structured emission at 620 and 670 nm was switched on at high concentration of Hg(II) ion (Figure 4 (right)). The close resemblance of the emission intensity changes at 620 nm (Figure 4 (right, inset)) and the absorbance changes at 593 nm (Figure 4, (left, inset)) as a function of Hg(II) ion concentrations is suggestive of the same origin, arising as a result of the second ring-opening process. This was further confirmed by the observation of excitation bands at about 546 and 593 nm in the excitation spectrum. The vibronic-structured emission showed a mirror image as the absorption band (Supporting Information, Figure

S4), typical of fluorescence nature as observed in other organic fluorophores, such as BODIPY, rhodamine, and fluorescein. Arising from two successive ring-opening processes in the presence of various concentrations of Hg(II) ion, two reporting states with different spectroscopic properties were suggested, that is, the first state showing pink color (absorption maximum at 496 nm) but no emission, while the second state showing purple color (absorption maximum at 593 nm) and red emission (emission maximum at 620 nm). The mechanism of such different spectroscopic responses is proposed in Scheme 4 (See Computational Studies). In the first reporting state with only one ring-opened spirolactam group, there is a π -conjugation across of three fused rings of a xanthene moiety and a phenyl group, which is responsible for the pink color and the absorption bands at 464, 496, and 530 nm. One would anticipate observing the corresponding emission attributed to

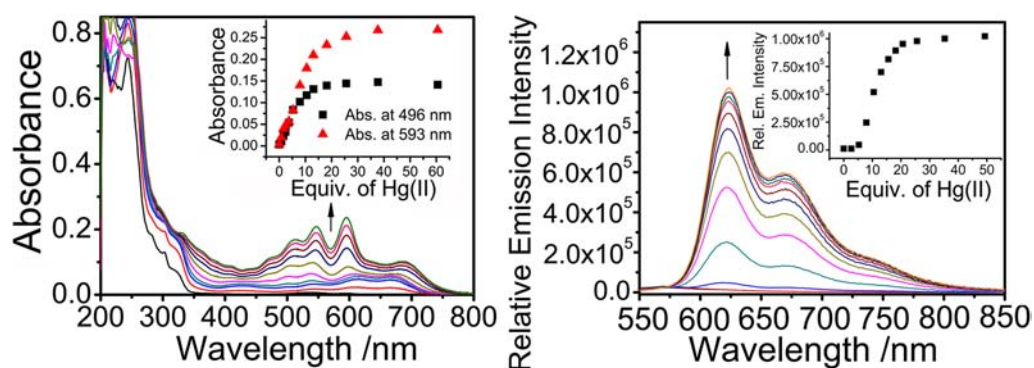


Figure 6. Electronic absorption (left) and emission (right) spectral changes of *trans-2* (conc. = 9.57×10^{-6} M) upon addition of various concentrations of Hg(II) ion in MeOH. Insets show the plot of absorbance or emission intensity as a function of the concentration of Hg(II) ion.

such π -conjugated structure, similar to that of the ordinary rhodamine derivatives. However, no detectable emission was observed in this reporting state, probably because of the PET process from another diethylamino group. In the second reporting state with two ring-opened spirolactam groups in the presence of a higher concentration of Hg(II) ions, a higher extended π -conjugation across the fused-structure of five rings and two phenyl groups is suggested to give the purple color and the absorption bands at 546 and 593 nm. An intense vibronic-structured emission at 620 and 670 nm emerged, which is attributed to this higher extension of the π -conjugated structure. In this reporting state, the aforementioned PET process was blocked with no available lone pair electron since both of the two electron-donating diethylamino groups were converted into electron-deficient ammonium groups.

The spectroscopic changes of **2** upon addition of Hg(II) ion have also been investigated and are basically similar to those of **1**. The corresponding electronic absorption spectral changes of *cis-2* in methanol are illustrated in Figure 5 (left). In view of the observation of the 593 nm absorption band (Figure 5 (left)) and 620 nm emission peak (Figure 5 (right)), successive ring-opening processes upon addition of Hg(II) ion were also demonstrated (Scheme 4). The growth of absorbance or emission intensity exhibits a sigmoid response curve and reaches saturation at relatively low concentration of Hg(II) ion of about 7 mol equiv. It was suggested that the two amide groups in *cis*-orientation would cooperatively bind one Hg(II) ion leading to the ease of the second ring-opening process. Upon addition of Hg(II) ion into the solution of *trans-2*, the change of solution color and emission intensity is slightly different from those of *cis-2*. In addition to the absorption bands at 496 and 593 nm, the electronic absorption spectra of *trans-2* with excess Hg(II) ion revealed that there is another low-energy absorption at 688 nm (Figure 6, (left)), which may account for the slight difference in the solution color. On the other hand, an emission band at 623 nm was also observed upon the ring-opening of two spirolactam groups (Figure 6, (right)). The emission intensity profile is consistent with the plot of the 593 nm absorbance to the function of Hg(II) ion concentration, which reaches the saturation at 25 equiv of Hg(II) ion. The discrepancies in their sensitivity and spectroscopic response toward Hg(II) ion between *cis-2* and *trans-2* indicate that the different conformations of stereoisomers in **2** would influence their ring-opening behaviors, which is in contrast to the case of **1**. As ring-opening of the spirolactam of rhodamine derivatives is commonly induced by protonation,⁶ successive ring-opening processes with the similar

spectroscopic changes were also observed for *cis-1* (Supporting Information, Figure S5) or *trans-1* (Supporting Information, Figure S6) upon addition of acid. Unlike **1**, addition of small amount of acid resulted in no observable solution color and spectroscopic changes for **2**, mainly because of the presence of two other NH₂ groups. This result shows the advantage of compound **2** to selectively sense Hg(II) ion without the interference of acid.

Chemodosimeter Studies. The research of selective chemosensors for toxic heavy metal ions for the detection of environmentally and biologically species has been developed largely in recent years.^{3b,c,6c,8a} A rhodamine-based chemodosimeter for Hg(II) ion was first reported by Tae and co-workers in 2005,^{8a} in which a stoichiometric and irreversible Hg(II)-promoted reaction of thiosemicarbazides was utilized to form 1,3,4-oxadiazoles leading to the concept of selective Hg(II) ion colorimetric and fluorescent chemodosimeters.⁹ To extend the work to study the corresponding chemodosimeters from the present compound with two spirolactam groups, a related compound *cis-3* was synthesized (Scheme 2). An optimized condition of acetonitrile-buffer (1:1, v/v), in which the buffer was HEPES buffer solution (pH = 7.0, 10 mmol) in water, as the solvent was used. Upon addition of Hg(II) ion into the solution of *cis-3*, an instantaneous color change from colorless to purple was observed, indicating that the Hg(II) ion mediated desulfurization reaction proceeded rapidly at room temperature. No such color change or only very small color change was observed upon addition of various ions, including Li⁺, Na⁺, K⁺, Ca²⁺, Mg²⁺, Ba²⁺, Zn²⁺, Cd²⁺, Ag⁺, Cu²⁺, Pb²⁺, F⁻, Cl⁻, and I⁻, suggestive of the high selectivity toward Hg(II) ion (Supporting Information, Figure S7). In view of the presence of two thiosemicarbazides undergoing desulfurization reaction in *cis-3*, the time required for the complete reaction may be longer than the related simple rhodamine compounds. It was found that the electronic absorption spectrum of *cis-3* remained the same after 30 min upon addition of about 1.8 equiv of Hg(II) ion. A 30-min reaction time was therefore selected in the subsequent spectroscopic experiments. Electronic absorption titration studies of *cis-3* with various concentrations of Hg(II) ion were also carried out. Similar to the cases in **1** and **2** (both in *trans*- and *cis*-forms), two successive ring-opening processes were indicated from the spectroscopic profile (Figure 7). The absorbance at 602 nm, which corresponds to the extended π -conjugated structure after the second ring-opening of spirolactam groups, emerged, and the formation of **4** (Scheme 5) in this solution upon addition of Hg(II) ion was identified by mass spectroscopy showing prominent peaks at $m/z = 448.3$

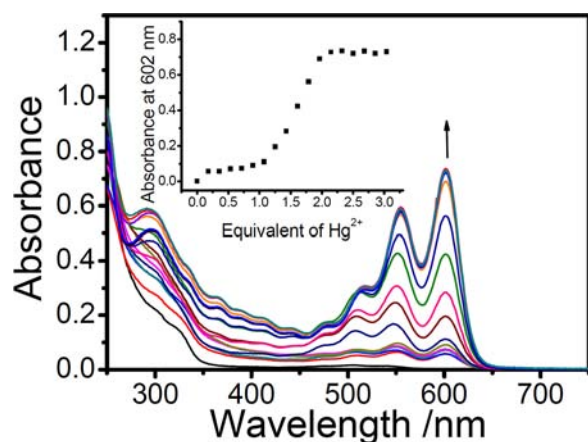


Figure 7. Electronic absorption spectral changes of *cis-3* (conc. = 12×10^{-6} M) upon addition of increasing concentrations of Hg(II) ion in acetonitrile-buffer (1:1, v/v) solution. (buffer = HEPES buffer solution (pH = 7.0, 10 mmol) in water).

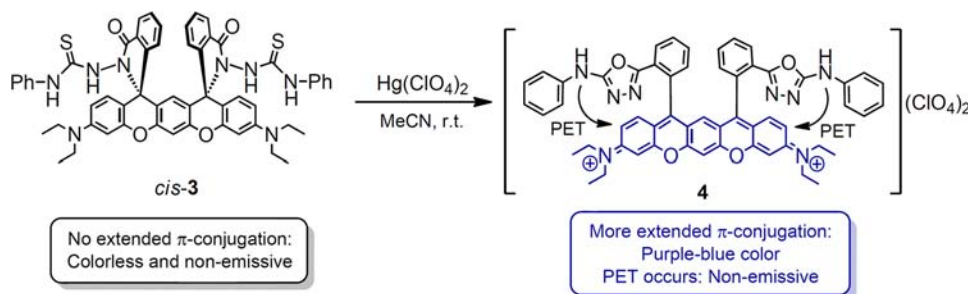
$[M]^{2+}$ and $895.3 [M - H]^+$. The formation of **4** from *cis-3* and Hg(II) ion was further confirmed by comparing the electronic absorption spectra of *cis-3* and Hg(II) ion mixture, and pure **4** (Supporting Information, Figure S8) prepared independently. Such absorbance at 602 nm reached to a saturation in 2 equiv of Hg(II) ion revealing the Hg(II) ion chemodosimeter in 1:2 stoichiometry. However, no detectable emission was observed, probably because of the PET process from the $-(C_2N_2O)-NH(C_6H_5)$ groups (Scheme 5) (See Computational Studies). A similar PET process leading to emission quenching behavior has also been reported.^{3b,6c} Selectivity and interference studies were also performed by monitoring the absorbance at 602 nm in the solutions of *cis-3* containing various ions (Supporting Information, Figure S9). Apart from the remarkably high selectivity toward Hg(II) ion, such colorimetric response will not be influenced by subsequent addition of other metal ions. When the resulting colored solution was subsequently treated with 0.5 mol/L EDTA solution, the absorbance signal at 602 nm remained almost unchanged, indicative of the occurrence of irreversible desulfurization reaction.

Computational Studies. To explore the feasibility of PET in the present system, density functional theory (DFT) calculations were performed, on the basis of the proposed structures of the partial and full ring-opened form of **1**, with one and two ring-opened spiro lactam group(s) on the carboxylic acid, respectively. As shown in Figure 8 (left), the highest occupied molecular orbital (HOMO) of the partial ring-opened *cis-1* (*cis-1-p*) was localized on the diethylamino group and the benzene ring linked directly to the ring-closed

xanthene moiety. The energy level of the HOMO was found between those of the lowest unoccupied molecular orbital (LUMO) with the ring-opened xanthene character and the HOMO-1 with the five fused rings character, indicating that the diethylamino group could act as potential electron donor of the proposed PET process for the emission originated from HOMO-1 and LUMO excited state, accounting for the nonemissive behavior of partial ring-opened *cis-1* (*cis-1-p*). In contrast, both of the HOMO and LUMO of the full ring-opened *cis-1* (*cis-1-f*) were found to locate at the five fused rings of the luminophore (Figure 8 (right)), which demonstrates that there is no electron donor for the PET process, and red fluorescence was therefore observed. Similar PET from a deprotonated tertiary amine N-oxide moiety was suggested by DFT calculations for the nonradiative deactivation of the emitting process of the chromophore in the related rhodamine-based fluorescent probe.⁸¹ The DFT calculation results for *trans-1* were similar to that for *cis-1* (Supporting Information, Figure S10). TD-DFT calculations on the absorption spectra in methanol were also carried out to further understand the electronic transitions. As listed in Supporting Information, Table S2 and shown in Supporting Information, Figure S11, an intense absorption peak at 471 nm ($f = 1.0346$) for the partial ring-opened *cis-1* (*cis-1-p*) and at around 535 nm ($f = 1.3279$) for the full ring-opened *cis-1* (*cis-1-f*) were calculated, which were ascribed to the strong xanthene-centered $n \rightarrow \pi^*$ transition (HOMO-1 \rightarrow LUMO) and the $n \rightarrow \pi^*$ transition centered at the five fused rings (HOMO \rightarrow LUMO), respectively. The drastic red-shift in the absorption band from 471 to 535 nm was responsible for the color change from pink to purple in the solution of *cis-1* upon further addition of Hg(II) ions. Such red-shift in the absorption band was in agreement with the experimental results in electronic absorption spectroscopy and ascribed to the increase in the extended π -conjugation from xanthene to five fused rings.

In contrast to the similar structure of the full ring-opened forms of **1** and **2**, it is interesting to note that compound **4**, with two ring-opened spiro lactam groups, was found to show nonemissive behavior. The frontier molecular orbital energies and electron density distributions of **4** were shown in Figure 9 (left). Five molecular orbitals (from HOMO to HOMO-4) located at one of the $-(C_2N_2O)NH(C_6H_5)$ groups or their phenyl were found between the frontier molecular orbitals of the five fused rings chromophore (HOMO-5 and LUMO). The $-(C_2N_2O)NH(C_6H_5)$ groups were suggested to act as electron donors of the proposed PET process, responsible for nonradiative deactivation of the excited state of **4**. On the other hand, a closely related simple rhodamine 6G_oxadiazole was reported by Tae and co-workers to give intense fluorescence at

Scheme 5. Proposed Mechanism for the Color Changes and Emission Behaviors of *cis-3* and **4**



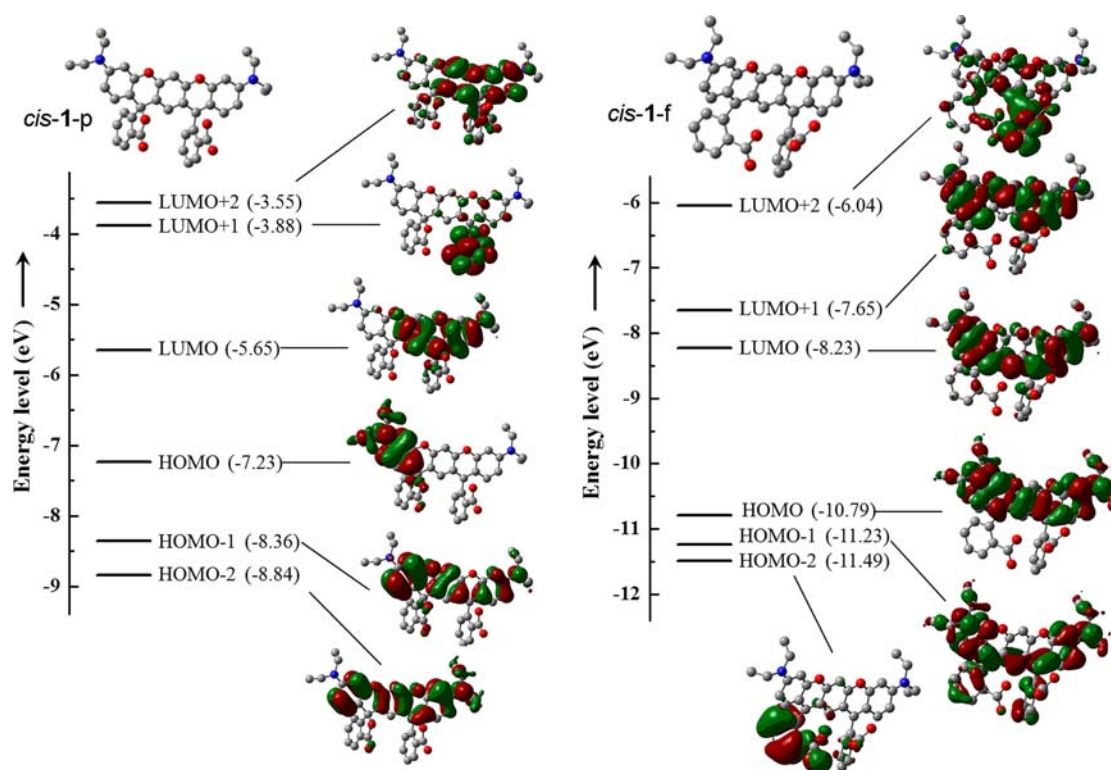


Figure 8. Optimized ground state geometries, frontier molecular orbital energies and electron density distributions of *cis-1-p* (left) and *cis-1-f* (right).

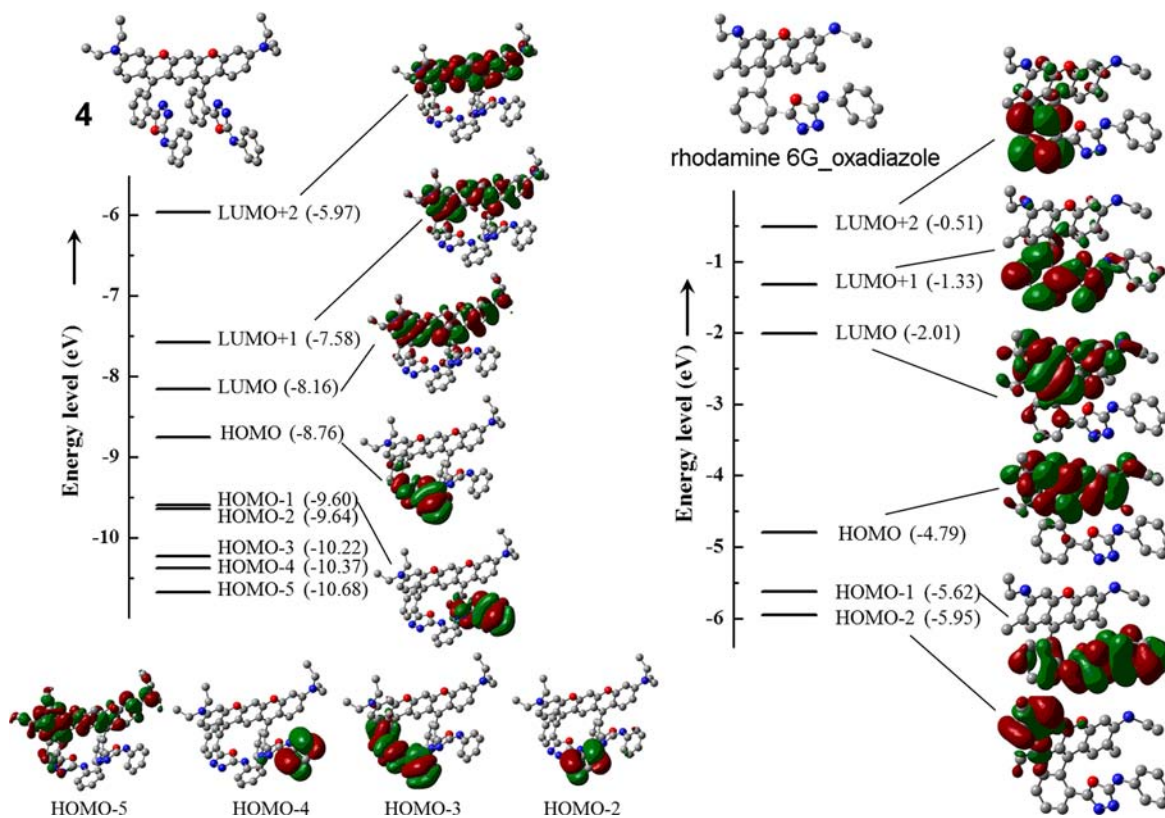


Figure 9. Optimized ground state geometries, frontier molecular orbital energies, and electron density distributions of **4** (left) and rhodamine 6G_oxadiazole (right).

around 555 nm in water–methanol (4/1 v/v, pH = 7).^{8a} DFT calculations were also performed on such system, and the

molecular orbitals with $-(C_2N_2O)NH(C_6H_5)$ character were lower in energy than the HOMO with xanthen character

(Figure 9 (right)). The absence of an electron donor for the fluorescence quenching in the PET process elucidated the intense fluorescence in rhodamine 6G_oxadiazole. TD-DFT calculations on the absorption spectra of **4** and rhodamine 6G_oxadiazole were also performed, as shown in Supporting Information, Figure S11 and Table S2.

CONCLUSION

In conclusion, a novel class of rhodamine derivatives with two spirolactam groups and five fused six-membered rings were synthesized, and their stereoisomers of *cis*- and *trans*-forms were successfully separated and isolated. Compared to the related rhodamine B base and rhodamine B hydrazide with only one spirolactam group, derivatives **1** or **2** with two binding sites were found to exhibit selective Hg(II) ion sensing behaviors. Successive ring-openings of two spirolactam moieties were demonstrated to show drastic color changes and emission enhancement in their solution mixture of Hg(II) ion. The extension of the π -conjugation across the fused-structure of five rings shifts the absorption and emission to the red, compared with those of common rhodamine derivatives. Compound **2** showed the selective sensing to Hg(II) ion without the interference of acid, and different conformations in their stereoisomers were found to influence the ring-opening behaviors differently. Arising from two successive ring-opening processes in the presence of various concentration of Hg(II) ion, two reporting states with different spectroscopic properties were suggested, that is, the first state showing pink color (absorption maximum at 496 nm) but no emission, while the second giving purple color (absorption maximum at 593 nm) and red emission (emission maximum at 620 nm). The mechanism of such different spectroscopic responses was also proposed, which has also been supported by computational studies. An extension of the present work to the study of corresponding chemodosimeters from the compounds with two spirolactam groups has been made, in which an stoichiometric and irreversible Hg(II)-promoted reaction of thiosemicarbazides was utilized to form 1,3,4-oxadiazoles.

ASSOCIATED CONTENT

Supporting Information

X-ray crystallographic data of *cis*-**1**, *trans*-**1**, *cis*-**2**, and *trans*-**2** in CIF format. Structures of *cis*-**1**, *trans*-**1**, *cis*-**2**, and *trans*-**2**, titration spectral changes with Hg(II) ion and acid, and other related DFT and TDDFT results. This material is available free of charge via the Internet at <http://pubs.acs.org>.

AUTHOR INFORMATION

Corresponding Author

*E-mail: keithwongmc@sustc.edu.cn.

Notes

The authors declare no competing financial interest.

ACKNOWLEDGMENTS

K.M.C.W. acknowledges the receipt of "Young Thousand Talents Program" award and the start-up fund administrated by the Organisation Department of CPC Central Committee and South University of Science and Technology of China, respectively. We gratefully thank Dr. L. Szeto and Prof. W.T. Wong for X-ray crystal structure determinations, Dr. J. Weng for computational studies, and Prof. V.W.W. Yam for access to

the equipment for photophysical measurements and for her helpful discussions.

REFERENCES

- (1) (a) Pedersen, C. J. *J. Am. Chem. Soc.* **1967**, *89*, 7017. (b) Pedersen, C. J.; Lehn, J. M. *Angew. Chem., Int. Ed. Engl.* **1988**, *27*, 1021. (c) Cram, D. J. *Angew. Chem., Int. Ed. Engl.* **1988**, *27*, 1009.
- (2) (a) Elghanian, R.; Storhoff, J. J.; Mucic, R. C.; Letsinger, R. L.; Mirkin, C. A. *Science* **1997**, *277*, 1078. (b) Göpel, W. *Mikrochim. Acta* **1997**, *125*, 179. (c) Gvpel, W. *Microelectron. Eng.* **1996**, *32*, 75. (d) Zhu, S. S.; Carroll, P. J.; Swager, T. M. *J. Am. Chem. Soc.* **1996**, *118*, 8713.
- (3) (a) Czarnik, A. W. *Fluorescent Chemosensors for Ion and Molecular Recognition*; American Chemical Society: Washington, DC, 1993. (b) de Silva, A. P.; Gunaratne, H. Q. N.; Gunnlaugsson, T.; Huxley, A. J. M.; McCoy, C. P.; Rademacher, J. T.; Rice, T. E. *Chem. Rev.* **1997**, *97*, 1515. (c) Valeur, B.; Leray, I. *Coord. Chem. Rev.* **2000**, *205*, 3. (d) Martínez-Máñez, R.; Sancenón, F. *Chem. Rev.* **2003**, *103*, 4419.
- (4) (a) Bryan, A. J.; de Silva, A. P.; de Silva, S. A.; Rupasinghe, R. A. D. D.; Sandanayake, K. R. A. S. *Biosensors* **1989**, *4*, 169. (b) Woodroffe, C. C.; Lippard, S. J. *J. Am. Chem. Soc.* **2003**, *125*, 11458. (c) Kim, S. K.; Lee, S. H.; Lee, J. Y.; Bartsch, R. A.; Kim, J. S. *J. Am. Chem. Soc.* **2004**, *126*, 16499. (d) Kim, S. K.; Kim, S. H.; Kim, H. J.; Lee, S. H.; Lee, S. W.; Ko, J.; Bartsch, R. A.; Kim, J. S. *Inorg. Chem.* **2005**, *44*, 7866. (e) Zhang, G.; Zhang, D.; Yin, S.; Yang, X.; Shuai, Z.; Zhu, D. *Chem. Commun.* **2005**, 2161. (f) Métivier, R.; Leray, I.; Lebeau, B.; Valeur, B. *J. Mater. Chem.* **2005**, *15*, 2965. (g) Coronado, E.; Galan-Mascaros, J. R.; Marti-Gastaldo, C.; Palomares, E.; Durrant, J. R.; Vilar, R.; Grätzel, M.; Nazeeruddin, Md. K. *J. Am. Chem. Soc.* **2005**, *127*, 12351. (h) Lee, S. J.; Jung, J. H.; Seo, J.; Yoon, I.; Park, K.-M.; Lindoy, L. F.; Lee, S. S. *Org. Lett.* **2006**, *8*, 1641. (i) Nazeeruddin, M. K.; Di Censo, D.; Humphry-Baker, R.; Grätzel, M. *Adv. Funct. Mater.* **2006**, *16*, 189. (j) Liu, L.; Zhang, G.; Xiang, J.; Zhang, D.; Zhu, D. *Org. Lett.* **2008**, *10*, 4581.
- (5) (a) Noelting, E.; Dziewonsky, K. *Ber. Dtsch. Chem. Ges.* **1905**, *38*, 3516. (b) Valeur, B. *Molecular Fluorescence: Principles and Applications*; Wiley-VCH: New York, 2001; Chapter 10.
- (6) For some reviews and examples: (a) Kim, H. N.; Lee, M. H.; Kim, H. J.; Kim, J. S.; Yoon, J. *Chem. Soc. Rev.* **2008**, *37*, 1465. (b) Beija, M.; Afonso, C. A. M.; Martinho, J. M. G. *Chem. Soc. Rev.* **2009**, *38*, 2410. (c) Quang, D. T.; Kim, J. S. *Chem. Rev.* **2010**, *110*, 6280.
- (7) (a) Dujols, V.; Ford, F.; Czarnik, A. W. *J. Am. Chem. Soc.* **1997**, *119*, 7386. (b) Kwon, J. Y.; Jang, Y. J.; Lee, Y. J.; Kim, K. M.; Seo, M. S.; Nam, W.; Yoon, J. *J. Am. Chem. Soc.* **2005**, *127*, 10107.
- (8) (a) Yang, Y. K.; Yook, K. J.; Tae, J. *J. Am. Chem. Soc.* **2005**, *127*, 16760. (b) Zheng, H.; Qian, Z.-H.; Xu, L.; Yuan, F.-F.; Lan, L.-D.; Xu, J.-G. *Org. Lett.* **2006**, *8*, 859. (c) Choi, M. G.; Ryu, D. H.; Jeon, H. L.; Cha, S.; Cho, J.; Joo, H. H.; Hong, K. S.; Lee, C.; Ahn, S.; Chang, S.-K. *Org. Lett.* **2008**, *10*, 3717. (d) Suresh, M.; Shrivastav, A.; Mishra, S.; Suresh, E.; Das, A. *Org. Lett.* **2008**, *10*, 3013. (e) Wu, D.; Huang, W.; Duan, C.; Lin, Z.; Meng, Q. *Inorg. Chem.* **2007**, *46*, 1538. (f) Mao, J.; Wang, L.; Dou, W.; Tang, X.; Yan, Y.; Liu, W. *Org. Lett.* **2007**, *9*, 4567. (g) Atanu, J.; Kim, J. S.; Jung, H. S.; Parimal, K. B. *Chem. Commun.* **2009**, 4417. (h) Wang, C.; Wong, K. M. C. *Inorg. Chem.* **2011**, *50*, 5333. (i) Hirayama, T.; Okuda, K.; Nagasawa, H. *Chem. Sci.* **2013**, *4*, 1250.
- (9) (a) Wu, J. S.; Hwang, I. C.; Kim, K. S.; Kim, J. S. *Org. Lett.* **2007**, *9*, 907. (b) Zhang, X.; Xiao, Y.; Xiao, Y.; Qian, X. *Angew. Chem., Int. Ed.* **2008**, *47*, 8025. (c) Zhang, J. F.; Lim, C. S.; Cho, B. R.; Kim, J. S. *Talanta* **2010**, *83*, 658.
- (10) Frisch, M. J.; Trucks, G. W.; Schlegel, H. B.; Scuseria, G. E.; Robb, M. A.; Cheeseman, J. R.; Scalmani, G.; Barone, V.; Mennucci, B.; Petersson, G. A.; Nakatsuji, H.; Caricato, M.; Li, X.; Hratchian, H. P.; Izmaylov, A. F.; Bloino, J.; Zheng, G.; Sonnenberg, J. L.; Hada, M.; Ehara, M.; Toyota, K.; Fukuda, R.; Hasegawa, J.; Ishida, M.; Nakajima, T.; Honda, Y.; Kitao, O.; Nakai, H.; Vreven, T.; Montgomery, J. A., Jr.; Peralta, J. E.; Ogliaro, F.; Bearpark, M.; Heyd, J. J.; Brothers, E.; Kudin, K. N.; Staroverov, V. N.; Kobayashi, R.; Normand, J.;

Raghavachari, K.; Rendell, A.; Burant, J. C.; Iyengar, S. S.; Tomasi, J.; Cossi, M.; Rega, N.; Millam, J. M.; Klene, M.; Knox, J. E.; Cross, J. B.; Bakken, V.; Adamo, C.; Jaramillo, J.; Gomperts, R.; Stratmann, R. E.; Yazyev, O.; Austin, A. J.; Cammi, R.; Pomelli, C.; Ochterski, J. W.; Martin, R. L.; Morokuma, K.; Zakrzewski, V. G.; Voth, G. A.; Salvador, P.; Dannenberg, J. J.; Dapprich, S.; Daniels, A. D.; Farkas, O.; Foresman, J. B.; Ortiz, J. V.; Cioslowski, J.; and Fox, D. J. *Gaussian 09*, Revision A.01; Gaussian, Inc.: Wallingford, CT, 2009.

(11) Compound **1** has previously been reported without successful separation and isolation of the diastereomers. Kamino, S.; Horio, Y.; Komeda, S.; Minoura, K.; Ichikawa, H.; Horigome, J.; Tatsumi, A.; Kaji, S.; Yamaguchi, T.; Usami, Y.; Hirota, S.; Emomoto, S.; Fujita, Y. *Chem. Commun.* **2010**, *46*, 9013.

(12) Although some of the refinement R-factors are large resulting from the low completeness of data collection probably because of the poor quality of single crystals, the assignment of stereoisomers for *cis*- and *trans*-forms could be definitely confirmed.